Book of Tutorials and Abstracts


European Microbeam Analysis Society

# EMAS 2023

**17th**

**EUROPEAN WORKSHOP**

**on**

# MODERN DEVELOPMENTS AND APPLICATIONS IN MICROBEAM ANALYSIS

7 to 11 May 2023
at the
Jagiellonian University, Auditorium Maximum
Krakow, Poland

Under the auspices of the Rector of the
Jagiellonian University, Krakow, Poland
Organised in collaboration with the
Institute of Metallurgy and Materials Science of
the Polish Academy of Sciences, Krakow, Poland

*EMAS*
European Microbeam Analysis Society eV
www.microbeamanalysis.eu/

This volume is published by:
European Microbeam Analysis Society eV (EMAS)
EMAS Secretariat
c/o Eidgenössische Technische Hochschule, Institut für Geochemie und Petrologie
Clausiusstrasse 25
8092 Zürich
Switzerland



ISBN 978 90 8227 6961
NUR code: 972 – Materials Science

# BADGERFILM: A NEW THIN FILM ANALYSIS PROGRAMME (WITH OTHER USEFUL APPLICATIONS) FOR EPMA

Aurélien Moy and J.H. Fournelle

University of Wisconsin, Department of Geoscience
US-53706 Madison, WI, U.S.A.
e-mail: amoy6@wisc.edu

Aurélien Moy is a researcher at the Geoscience Department of the University of Wisconsin-Madison. He specialises on developing new EPMA methods for quantification using soft X-rays at low accelerating voltages.

Aurélien received his engineering degree in Electronics and Applied Physics, with a specialty in Nuclear Engineering, from the National Graduate School of Engineering & Research Centre of Caen (ENSICAEN), France in 2011. He earned his PhD in Geoscience/Physics from the University of Montpellier, and the French Alternative Energies and Atomic Energy Commission (CEA) research centre of Marcoule, in 2014. Aurélien's thesis received the European Microbeam Analysis Society Thesis Award in 2015 for his work on the measurement of atomic parameters of actinides and the development of standardless quantification methods of actinides by EPMA. After his PhD, he worked at the CEA research centre of Cadarache, France, before joining UW-Madison as a Postdoc.

Aurélien has authored over 30 publications and conference proceedings on EPMA. He has been recognised with several awards, including the Young Scientist Award from the European Microbeam Analysis Society in 2013, the Early Career Scholar Award from the International Union of Microbeam Analysis Societies in 2014 and 2017, and the Microanalysis Society Macres Award for best instrumentation/software in 2020.

## 1. ABSTRACT

Characterisation of thin films upon substrates, i.e., thickness and composition determination, can be performed using the non-destructive technique of electron probe microanalysis (EPMA). This technique, first introduced in the 1960's and refined in the 1990's, is based on the accurate description of the electron ionisation depth distribution, the so-called $\phi(\rho z)$ distribution. Using these models, several thin film analysis computer programmes have been developed and distributed. However, these programmes have some limitations: (1) older programmes may not be compatible with modern computer systems, (2) the majority of the programmes are "black boxes" making difficult to assess the reliability of the quantification results, and (3) commercial programmes can be expensive and this might prevent a lab from acquiring one of them especially when demands for thin film quantification are occasional. And experience has shown that where an EPMA lab is searching for funds and new users/customers, the ability to do thin film characterisation can be valuable.

In this article, we present the thin film analysis programme BADGERFILM. The programme is free, open-source and implements documented $\phi(\rho z)$-model and algorithms. The programme is versatile and can be used to characterise multi-layer samples but also bulk samples. BADGERFILM demonstrated excellent quantification results for the films and for the substrates when compared to other EPMA thin film analysis programmes and to other techniques. BADGERFILM can also be employed to calculate mass absorption coefficients from multi-voltage EPMA measurements and can calculate absolute X-ray intensities directly comparable to Monte Carlo simulations.

## 2. INTRODUCTION

Thin film materials are found in numerous modern technologies. They are employed, for example, in optical coatings to form anti-reflecting materials using multiple layers with varying thicknesses and refractive indices. Thin films are also used in electronic semiconductor devices, magnetic storage, superconductor research, etc. The direct characterisation of sub-micrometre to nanometre films requires specialised equipment's and techniques [1]. The use of the electron microprobe for the analysis of thin films was soon recognised after the development of the technique by Raimond Castaing [2, 3]. The electron probe technique was not originally designed to analyse thin film specimens, mainly because the early matrix correction methods assumed a bulk homogeneous analytical volume. However, in the 1990's, with the development of realistic and accurate analytical descriptions of the depth distribution of the primary ionisations generated per incident electrons in the target -- the $\phi(\rho z)$ [phi-rho-Z] distribution, and hence improving the matrix corrections -- it became possible to use the technique for accurate thin film characterisation. The technique is now employed in a wide variety of fields to determine, for example, coating thicknesses, the presence of oxidation layers or thin film homogeneity [4]. The $\phi(\rho z)$-distribution is also commonly used to determine the composition of bulk homogeneous

specimens, i.e., having a thickness of at least several micrometres, greater than the X-ray analytical volume of the generated X-rays. Multiple $\phi(\rho z)$-models were developed over the years [5]. Among them, we can cite the models of Pouchou and Pichoir, PAP and XPP [6], and the model of Merlet, XPHI [7, 8], which are some of the most recent and most used models.

The characterisation of thin films (a single film on a substrate or a multi-layer specimen) cannot be performed using the traditional EPMA methods and software, which assume a bulk sample. It requires special procedures and data analysis techniques, the most common one used being the multi-voltage analysis method. This method consists of the measurement at several accelerating voltages of the *k*-ratios, i.e., the ratio of the X-ray intensity (corrected for the background and the dead-time and interferences) emitted by the element in question measured on both the unknown and on a standard material. The measured *k*-ratios are then compared to calculated (theoretical) *k*-ratios (obtained using a $\phi(\rho z)$-model appropriate for thin film determination) in which the thickness and/or the composition of the layers or substrate are the unknowns. By successive iterations on these values, theoretical *k*-ratios are calculated until their values closely match the experimental *k*-ratios. This analysis procedure requires dedicated thin film analysis programmes. Except for one of them, these programmes are commercially available at a relatively expensive cost (i.e., thousands of euros/dollars). Therefore, laboratories that only perform occasional thin film characterisation work may be hesitant to acquire them.

The only exception is GMRFILM, a free research-grade shareware DOS programme developed by R. Waldo at General Motors Research in the late 1980's [9]. Despite its great capabilities, GMRFILM suffers from its age and modern operating systems do not readily support it anymore, making its use difficult. The programme also only allows the analysis of *k*-ratios measured at one accelerating voltage at a time, losing the benefits of the multi-voltage analysis: In the case where no elements are simultaneously present in the different layers and the substrate, the characterisation can be performed using only one set of *k*-ratios measured at a single accelerating voltage. However, in practice several accelerating voltages are necessary to reduce the errors introduced by uncertainties on the experimental *k*-ratios and inaccuracies of the $\phi(\rho z)$-model.

The majority of the thin film analysis programmes are "black boxes" making it difficult to understand the algorithms used to generate the results and hence the accuracy of the results.

To remedy to this lack of free and transparent thin film analysis software, we present BADGERFILM, a free open-source EPMA thin film analysis program. BADGERFILM implements some of the most used $\phi(\rho z)$-models: the PAP, XPP and XPHI models. The convergence on the *k*-ratios is done by a non-linear fitting procedure based on the Levenberg-Marquardt algorithm [10, 11], ensuring the finding of a realistic solution even if the starting conditions (the necessary initial guess of the thicknesses and compositions) are far from the final results. BADGERFILM also offers the possibility to calculate and take into account the secondary fluorescence produced by characteristic X-rays and by the bremsstrahlung in the calculations. To calculate absolute X-ray intensities, the programme also implements some of the most recent atomic parameters

such as the mass absorption coefficients, and the electron impact ionisation cross-sections. Different models of atomic parameters can be selected by the user. BADGERFILM is written in .NET Visual Basic, is open source and can be freely downloaded at the following address: https://github.com/Aurelien354/BadgerFilm.

## 2. *X-RAY GENERATION*

To analyse thin films by EPMA, an accurate description of the primary electron ionisation distribution is necessary. The $\phi(\rho z)$-distribution is used to calculate the primary X-ray intensities generated in the sample and emitted outside the sample. The distribution is also used to calculate the secondary fluorescence generated by the primary characteristic X-rays. Finally, this distribution can also be adapted to calculate the secondary fluorescence created by the bremsstrahlung.

### 2.1. *Primary characteristic X-rays*

In the general case of a layer buried in a multi-layered sample, the primary X-ray intensity $I_i^s$ emitted by an element $i$ in the layer $s$ located between mass depth $\rho z_s$ and $\rho z_{s+1}$ can be expressed by:

$$I_i^s = n_{\mathrm{el}} \frac{N_A}{A_i} C_i \omega_j p_i \lambda_j \sigma_j(E_0) T_i^s \int_{\rho z_s}^{\rho z_{s+1}} \phi_j(\rho z)\, e^{-\chi_i^s (\rho z - \rho z_s)}\, d\rho z\ \varepsilon \frac{\Omega}{4\pi} \qquad (1)$$

where $n_{\mathrm{el}}$ is the number of incident electrons of energy $E_0$ reaching the sample per second. $N_A$ is Avogadro's number, $A_i$ represent the atomic weight of element $i$, and $C_i$ the weight fraction of element $i$. Then follow the relaxation parameters. The atomic parameter $\omega_j$ describes the fluorescence yield of shell (or subshell) $j$. The term $p_i$ is the line fraction and is equals to $\Gamma_{j\text{-}k}/\Gamma_{j\text{-total}}$ where $\Gamma_{j\text{-}k}$ represents the radiative transition probability for an electron to make a transition from shell $k$ to shell $j$, and $\Gamma_{j\text{-total}}$ represents the total radiative width for all possible transitions to the $j$ shell. To take into account the fact that electron vacancies in the shell of interest can be created by migration of vacancies between subshells of the same shell through non-radiative transitions (Coster-Kronig and super-Coster-Kronig transitions), and between subshells of different, most inner, shells through radiative and non-radiative transitions, the enhancement factor $\lambda_j$ is introduced. This factor is also sometimes denoted $1+T_{CK}$. $\sigma_j(E_0)$ is the ionisation cross-section of the shell (or subshell) $j$ by electron impact of incident energy $E_0$. The detector characteristics are represented by the terms $\varepsilon$ and $\Omega/4\pi$, which are the intrinsic detection efficiency and the solid angle of collection of the detector, respectively. Note that when calculating the $k$-ratio, i.e., the ratio of the X-ray intensities measured on the unknown and on a standard under the same instrumental conditions, the electron impact ionisation cross-sections $\sigma_j(E_0)$ present outside of the integral (Eq. 1), as well as the relaxation parameters and the detector efficiency terms, cancel out between the numerator and the denominator.

The term $T_i^s$ describes the absorption of the emitted characteristic X-rays by the $l$ layers above the layer $s$ and is given by:

$$T_i^s = \prod_{l=1}^{s-1} e^{-\chi_i^l (\rho z_l - \rho z_{l-1})} \tag{2}$$

where $\chi_i^l$ is the reduced mass absorption coefficient:

$$\chi_i^l = \left(\frac{\mu}{\rho}\right)_i^l \frac{1}{\sin\theta} \tag{3}$$

with $\left(\frac{\mu}{\rho}\right)_i^l$ being the mass absorption coefficient (MAC) of the material constituting the layer $l$ for the relevant radiation produced by the element $i$. The term $\theta$ represent the take-off angle of the detector. The term $\chi_i^s$ in Eq. (1) is the reduced MAC for the layer $s$. In Eq. (2), the term $\rho z_l$-$\rho z_{l-1}$ corresponds to the mass thickness of layer $l$, hence $e^{-\chi_i^l (\rho z_l - \rho z_{l-1})}$ represents the absorption of primary characteristic X-rays in the layer $l$. In Eq. (1), $\phi_j(\rho z)$ represents the ionisation distribution of the shell $j$ of element $i$. The integral term is calculated analytically or numerically, depending on the $\phi_j(\rho z)$-model chosen, over the mass thickness of the layer (or substrate) $s$ to obtain the total emitted X-ray intensity.

However, $\phi(\rho z)$-distribution models must be adapted in the case of layered specimens. Indeed, as seen on Fig. 1, the ionisation depth distribution in a thin film on top of a substrate is different from the distribution in a bulk homogeneous specimen of the same material because of perturbating effects, such as the backscattered electrons from one layer to another. In the following, we briefly describe two $\phi(\rho z)$-models implemented in BADGERFILM, as well as their modifications to handle the case of layered specimens.

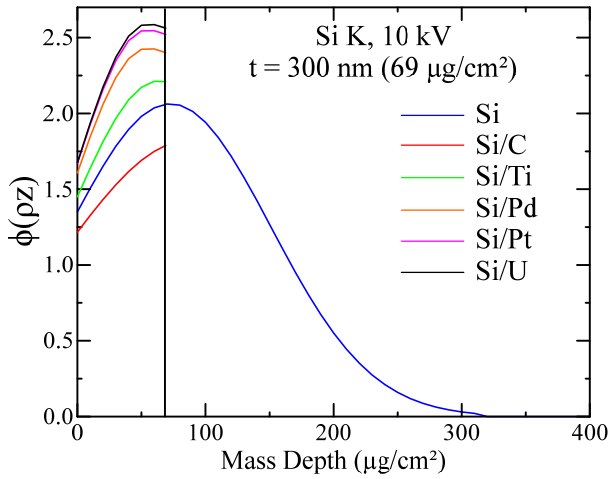


Figure 1. Effects of the substrate material (C, Ti, Pd, Pt or U) on the electron ionisation depth distribution of the K shell of Si by 10 keV primary electrons in a 300 nm-thick film of Si. The distribution in pure Si is also shown. When the atomic number of the substrate increases, the number of electrons backscattered into the film increases, leading to an increase of the $\phi(\rho z)$-distribution in the film. Results obtained with BADGERFILM using the XPHI model [8].

*2.2. The PAP model*

The PAP model was developed by Pouchou and Pichoir at the end of the 1980's [12, 13] and refined in the 1990's [6]. The model is based on the definition of the $\phi(\rho z)$-distribution given by Castaing [14] stating that the area of the $\phi(\rho z)$-distribution is proportional to the number of primary ionisations in the shell $j$ of element $i$, $N_j$, produced per incident electron:

$$N_j = \frac{C_i}{A_i} N_A \, \sigma_j(E_0) \int_0^\infty \phi_j(\rho z) \, d\rho z \tag{4}$$

Pouchou and Pichoir assumed that the number of primary ionisations can be obtained irrespective of the modelling process, using the so-called continuous electron deceleration approximation:

$$N_j = C_i \, \frac{N_A}{A_i} R \frac{1}{S} \tag{5}$$

where $R$ is the backscatter loss factor and $1/S$ is the stopping factor. Hence, we can write:

$$R \, \frac{1}{S} \, \frac{1}{\sigma_j(E_0)} = \int_0^\infty \phi(\rho z) \, d\rho z \tag{6}$$

The expressions to calculate the factors $R$, $1/S$ and $\sigma_j(E_0)$ are given elsewhere [5, 6, 15]. Eq. (6) imposes a condition on the area of the $\phi(\rho z)$-distribution, but not on its form. Pouchou and Pichoir choose to describe the ionisation depth distribution along the target mass depth using two connected parabolas, as shown on Fig. 2:

$$\phi(\rho z) = \begin{cases} A_1(\rho z - R_m)^2 + B_1 & for \; 0 < \rho z \leq R_c \\ A_2(\rho z - R_x)^2 & for \; R_c < \rho z < R_x \end{cases} \tag{7}$$

where $\rho z$ represents the mass depth, $R_m$, $R_c$ and $R_x$ are the mass depth at which the distribution reaches its maximum, the mass depth at which the two parabolas are connected, and the maximum mass depth at which the ionisation ceases, respectively. By imposing the continuity of $\phi(\rho z)$ in $R_c$ as well as the continuity of $\phi'(\rho z)$ (the derivative of $\phi(\rho z)$) also in $R_c$, the parameters in Eq. (7) can be determined:

$$A_1 = \frac{\phi(0)}{\left(R_m\left(R_c - R_x\left(\frac{R_c}{R_m} - 1\right)\right)\right)}, \; B_1 = \phi(0) - A_1 {R_m}^2, \; A_2 = A_1 \frac{R_c - R_m}{R_c - R_x} \tag{8}$$

where $\phi(0)$ is the surface ionisation, i.e., the value of the $\phi(\rho z)$-distribution at the surface of the sample. The expressions to calculate $A_1$, $A_2$, $B_1$ and $\phi(0)$ are given elsewhere [5, 6, 15].

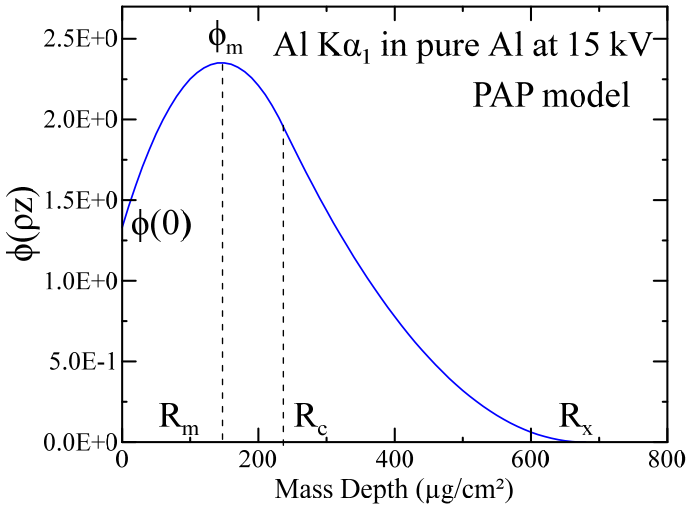


Figure 2. Si K ionisation depth distribution as a function of the mass depth calculated using the PAP model at 15 kV. The parameters of the $\phi(\rho z)$-distribution, $R_m$, $R_c$, $R_x$ and $\phi(0)$ are indicated.

To adapt the PAP model to the case of a layered specimen, a weighting equation is employed to generate a set of fictitious bulk compositions with which the form parameters $R_m$, $R_c$, $R_x$ and $\phi(0)$ are calculated. The weighting law used is a fourth order polynomial of the form [6, 16]:

$$p(\rho z, L_r, R_r) = N(\rho z - L_r)^2(\rho z - R_r)^2 \quad (9)$$

where $L_r$ and $R_r$ are the roots of Eq. (9) and are restricted to the interval $[-R_x; R_x]$. To constrain the area under p to be equal to 1 between 0 and $R_x$, the normalisation factor $N$ is employed. To each form parameter corresponds different values of $L_r$ and $R_r$ to give more or less weight to the first layer(s) of the stratified specimen and hence to give a better approximation of the associated form parameter. Using the appropriate values of $L_r$ and $R_r$, the fictitious concentrations $C_i^f$ of the $i$ elements composing a given layer (or the substrate) are calculated by:

$$C_i^f = C_i \times N \times \int_{\rho z_1}^{Min(\rho z_2; R_x)} p(\rho z, L_r, R_r)\, d\rho z \quad (10)$$

where $\rho z_1$ and $\rho z_2$ are the limits of the considered layer (or substrate) and $\rho z_2$ must not exceed the maximum mass depth ionisation $R_x$. Then, all the fictitious compositions, from the layers and the substrate, are summed and normalised to 100 wt% to create a fictitious bulk composition used to calculate the different parameters of the $\phi(\rho z)$-distribution. $R_x$ is calculated in an iteration loop with $R_r = R_x$ and $L_r = -0.4R_x$. To give more weight to the layers close to the surface, used for example to calculate $\phi(0)$, the roots $R_r = 0.5R_x$ and $L_r = -0.4R_r$ are used. $R_r = 0.7R_x$ and $L_r = -0.6R_r$ are used to calculate the deceleration factor $1/S$ used in the expression of $R_c$. $R_m$ is calculated using an average of the mean atomic numbers obtained during the calculations of $\phi(0)$ and $R_c$. See [6] or [16] for more details.

*2.3. The XPHI model*

The XPHI model was developed in the early 1990's by Merlet [17]. While the PAP model uses two connected parabolas to describe the $\phi(\rho z)$-distribution, the XPHI model uses a double-Gaussian distribution:

$$\phi(\rho z) = \begin{cases} \phi_m \, e^{-\frac{(\rho z - \rho z_m)^2}{\beta^2}} & for\ 0 < \rho z \leq \rho z_m \\ \phi_m \, e^{-\frac{(\rho z - \rho z_m)^2}{\alpha^2}} & for\ \rho z_m < \rho z \leq \rho z_x \end{cases} \quad (11)$$

with $\alpha = 0.46598\ (\rho z_x - \rho z_m)$ and $\beta = \frac{\rho z_m}{\sqrt{ln(\phi_m/\phi(0))}}$. As shown on Fig. 3, the XPHI model uses four form factors: $\phi(0)$ the surface ionisation, $\phi_m$ the maximum of the $\phi(\rho z)$-function, $\rho z_m$ the mass depth at which $\phi_m$ occurs, and $\rho z_x$ the mass depth at which the function becomes negligible ($\phi(\rho z_x) \leq 0.001$). The different expressions to calculate these form parameters are given elsewhere [5, 18]. The advantage of a description using Gaussian functions is that Eq. (1) can easily be integrated analytically:

$$I_i^s = cst\ n_{el}\ C_i\ T_i^s \frac{\sqrt{\pi}}{2} \phi_m \left\{ \beta e^{-\gamma} \left[ erf\left(\frac{\delta}{\beta}\right) + erf\left(\frac{\chi\beta}{2}\right) \right] + \alpha e^{-\zeta} \left[ 1 - erf\left(\frac{\chi\alpha}{2}\right) \right] \right\} \quad (12)$$

with $cst = \varepsilon\ \frac{\Omega}{4\pi}\ \frac{N_A}{A_i}\ \omega_j\ p_i\ \lambda_j\ \sigma_j(E_0)$, $\gamma = \rho z_m \chi - \left(\frac{\chi\beta}{2}\right)^2$, $\delta = \rho z_m - \frac{\chi\beta^2}{2}$, and $\zeta = \rho z_m \chi - \left(\frac{\chi\alpha}{2}\right)^2$. *Erf*(x) denotes the error function.

As described previously, for the case of multi-layer specimens, the $\phi(\rho z)$-distribution must be modified. The XPHI model, as implemented in XFILM [8], uses the weighting procedure originally introduced in [19] to calculate backscattering coefficients on thin films. The four form parameters are calculated using a hyperbolic tangent weighting function:

$$f_{F/S} = (f_F - f_S) \tanh(Ax + Bx^2) + f_S \quad (13)$$

where *f* denotes either of the form parameters. The subscript *F/S* denotes the form parameters calculated for the film over substrate specimen, and the subscripts *F* and *S* denote the form parameters calculated in a bulk sample with a composition similar to the film or substrate, respectively. The parameters *A* and *B* are given by:

$$A = \frac{2.153\ Z_F - 14.798}{3.706\ Z_F + 17.822} \quad , \quad B = \frac{0.3618\ Z_F - 27.80}{1.235\ Z_F - 82.055} \quad (14)$$

where $Z_F$ is the mean atomic number of the film: $Z_F = \sum_i C_i\ Z_i$ (with $C_i$ and $Z_i$ the concentration and the atomic number of the element *i*, respectively). The parameter *x* is a reduced thickness,

function of the mass thickness $t$ of the film and given by $x = 4t/(\rho z_x)$. The weighting function given by Eq. (13) ensures that for very thick films, the calculated form parameters are close to $f_F$ while for very thin films, the values tend toward $f_S$.

In the case of a multilayer specimen composed of $N$ layers on top of a substrate (the layer just on top of the substrate having the index $i = N$ and the layer at the surface of the sample having the index $i = 1$), the form parameters for the layer $i$ are given by Eq. (13) in which $f_F$ is replaced by the form factor of the layer $i$, $f_i$, and in which $f_S$ is replaced by the form factor of the layer $i$-1, $f_{i-1}$, i.e., the layer beneath the layer $i$. Practically, the form factors of the layer $N$ directly on top of the substrate must be calculated first using Eq. (13), and then the form factors of the layer $N$-1 can be calculated, etc. This process is repeated until the form factors of the layer at the surface (index $i = 1$) can be calculated. The parameters $A$, $B$ and $x$ are also calculated for each layer using the current layer's (layer $i$) composition and mass thickness.

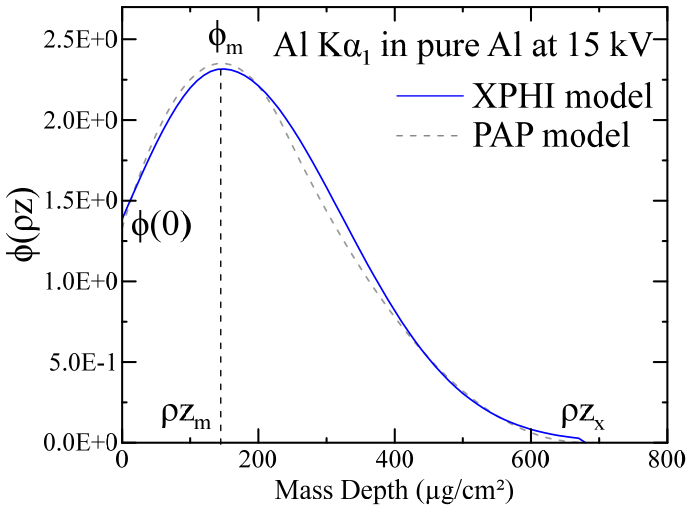


Figure 3. Si K ionisation depth distribution as a function of the mass depth calculated using the XPHI model at 15 kV. The parameters of the $\phi(\rho z)$-distribution, $\rho z_m$, $\rho z_x$, $\phi_m$ and $\phi(0)$ are indicated. The $\phi(\rho z)$-distribution from the PAP model is also displayed for comparison purpose. It is worth noting the two distributions are very similar.

### *2.4. Characteristic fluorescence*

The characteristic fluorescence is defined as the production of characteristic X-rays by other characteristic X-rays of higher energy. In some situations, the characteristic fluorescence can amount up to 30 % of the total X-ray intensity and should not be neglected. A classic example is the fluorescence of the Fe-Kα X-ray line by the Ni Kα- and Kβ-lines. At 25 kV, the Fe-Kα X-ray intensity of a 100 nm film of $FeSi_2$ deposited on a Ni substrate is increased by 9.5 % due to the characteristic fluorescence by Ni. The characteristic fluorescence is generally calculated numerically by considering all the characteristic X-rays with an energy higher than electron shell energy giving rise to the X-ray line of interest. These exiting characteristic X-rays come from all the other elements present in the electron interaction volume but also from the same element

producing the studied X-rays, e.g., the Fe-Lα X-rays can be excited by the Fe-Kα X-rays if these latter X-rays are produced. For each fluorescing X-ray line, the associated $\phi(\rho z)$-distribution is calculated, and the X-ray intensity calculated as a function of the mass depth. This latter function is then integrated along the mass depth of the relevant layer to calculate the fluorescence X-ray intensity. More details on the calculations can be found in [16].

### *2.5. Bremsstrahlung fluorescence*

The Bremsstrahlung fluorescence can amount up to a few percent of the total produced characteristic X-ray intensity. This effect increases as the difference between the measured characteristic X-ray and the electron beam energy increases because more Bremsstrahlung photons are available to excite the characteristic line of interest. This effect can be particularly important in thin films. A simple model to calculate the Bremsstrahlung fluorescence is to assume that the Bremsstrahlung X-rays are produced at a point on the surface of the considered layer [6]. A more refined model, as implemented in BADGERFILM, consists in calculating a $\phi(\rho z)$-distribution representative of the Bremsstrahlung distribution of energy $E_{ph}$. To the best of the authors' knowledge, there is no parametric model describing the Bremsstrahlung distribution as a function of the Bremsstrahlung energy $E_{ph}$. However, it is possible to approximate this distribution by using the PAP or XPHI $\phi(\rho z)$-models and by considering a fictitious element having a characteristic X-ray with a critical ionisation energy $E_{ph}$ equals to the energy of the considered bremsstrahlung photon. This distribution denoted $\phi_{Brem}(\rho z; E_{ph})$ represents the distribution of bremsstrahlung X-rays of energy $E_{ph}$ as a function of the mass depth $\rho z$ for a given material and electron beam energy. These $\phi(\rho z)$-distributions can then be integrated over the depth of the specimen to calculate fluorescence, following the same method as for the characteristic fluorescence. All the X-rays energies, from the electron beam energy $E_0$ down to the electron ionisation threshold of the characteristic X-ray of interest, $E_c$, as well as their associated $\phi_{Brem}$ distribution should be considered. In practice, the energy range $[E_c; E_0]$ is discretised into a finite subset of energies at which the $\phi_{Brem}$ distributions are calculated. This discretisation should also include the energy of the absorption edges of the elements constituting the specimen because the Bremsstrahlung X-ray spectrum (as a function of the photon energy) presents discontinuities at these energies. In each energy interval, the total emitted Bremsstrahlung fluorescence intensity is obtained by numerical integration.

However, the $\phi_{Brem}$ distributions obtained using the PAP or XPHI models are only an approximation of the real bremsstrahlung distribution. To help improve the model, the shape of the calculated X-ray spectrum (as a function of the photon energy) produced only by Bremsstrahlung fluorescence is weighted by the shape of the Bremsstrahlung spectrum $I(E)$ as proposed by Small *et al.* [20] and refined by Kulenkampff (as cited in [6]):

$$I(E) = q\, e^{B} \left[\bar{Z}\left(\frac{E_0}{E} - 1\right)\right]^{M} + C\, \bar{Z}^2 \qquad (15)$$

where $q$ is a scaling factor of $10^{-8}$ keV$^{-1}$ [6], B = $-3.22\times10^{-2}\times E_0+5.8$, M = $5.99\times10^{-3}\times E_0+1.05$ and C = $6\times0^{-10}$. The mean atomic number of the material $\bar{Z}$ is given by $\bar{Z} = \sum_i C_i Z_i$, where $C_i$ and $Z_i$ are quantities previously defined.

This method, despite producing more accurate results than the point surface method, appears to overestimate the Bremsstrahlung fluorescence intensity when compared to Monte Carlo simulations.

To improve the calculation of the Bremsstrahlung fluorescence, BADGERFILM implements two additional factors in Eq. (15):

$$I(E) = \beta(\bar{Z}) q\, e^{B\left[\bar{Z}\left(\frac{\alpha(\bar{Z})\,E_0}{E} - 1\right)\right]^M} + C\,\bar{Z}^2 \qquad (16)$$

where $\alpha(\bar{Z})$ modifies the energy of the primary electrons as a function of the mean atomic number of the material. This parameter is also introduced in the calculation of the Bremsstrahlung $\phi_{\text{Brem}}$ distribution and modifies the primary electron beam energy in a similar way. $\beta(\bar{Z})$ is a factor that modifies the value of the constant $q$. These parameters were obtained by adjusting their values until the calculated Bremsstrahlung fluorescence intensities match Bremsstrahlung fluorescence data obtained by Monte Carlo simulations using the code PENEPMA [21]. This fitting procedure was performed on pure elements using the main Kα, Lα, and Mα characteristic X-ray lines. The obtained values of $\alpha(\bar{Z})$ and $\beta(\bar{Z})$ can easily be fitted by part using polynomial functions, as seen in Fig. 4 for the Kα-line, with good coefficients of determination $R^2$. The obtained polynomials are implemented in BADGERFILM to calculate the Bremsstrahlung fluorescence.

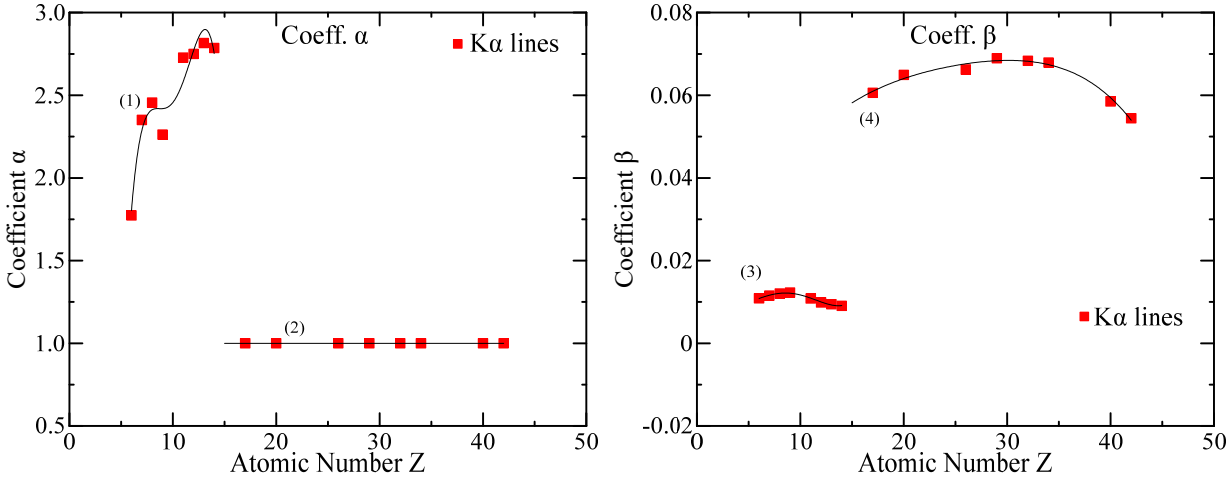


(1) y=-3.737141E-3x⁴ + 1.519312E-1x³ - 2.267005x² + 1.478875E1x - 3.329064E1; $R^2$=0.933
(2) y=1; $R^2$=1
(3) y=4.476461E-6x⁴ - 1.535630E-4x³ + 1.743002E-3x² - 7.318512E-3x + 1.937490E-2; $R^2$=0.991
(4) y=-1.153359E-7x⁴ + 1.138019E-5x³ - 4.570208E-4x² + 9.165271E-3x - 9.048994E-3; $R^2$=0.977

Figure 4. α- and β-coefficient values used in the calculation the Bremsstrahlung fluorescence for the Kα X-ray lines. Symbols are data obtained by fitting the coefficients to Monte Carlo simulations. Continuous lines represent the polynomial fits of the coefficients over the atomic number Z.

## 3. *BADGERFILM*

The described algorithms were implemented in BADGERFILM. The software is made of an open-source graphical user interface allowing fast and easy input and processing of the data to calculate thicknesses and compositions of multi-layered specimens. The programme can also be used to quantify bulk homogeneous samples in a traditional way and be employed to determine MAC-values using the multi-voltages method [22]. Multiple parameters can be selected such as the $\phi(\rho z)$-model, the MAC model or the ionisation cross-section model to use for quantification. The data required for quantification are the element symbol and its characteristic X-ray line, the associated experimental *k*-ratio, the accelerating voltage and optionally, the error on the *k*-ratio. The standard on which the *k*-ratio has been measured also needs to be specified by selecting a reference material, which the user has previously set up in BADGERFILM. In the case where the *k*-ratio was measured relative to a pure element, no standard needs to be specified. BADGERFILM can use traditional characteristic X-ray lines as well as less traditional lines: Kα (or Kα1, or Kα2), Kβ, Lα (or Lα1, or Lα2), Lβ1, Lγ1, Lη, Lℓ, L3N5, Mα1, Mα2, Mβ1, Mγ1, M4O6, M3O5, M2N4, M2N1, M3O1, M3O4, M1N2, M1N3, M2O4 and M1O2. To fit the data and converge towards a solution, BADGERFILM uses the Levenberg-Marquardt non-linear fitting method [10, 11] in which the compositions and thicknesses of the films (and substrate if so set) are varied until the calculated *k*-ratios matches the experimental *k*-ratios.

By default, BADGERFILM employs the same atomic parameters (relaxation parameters, MACs and ionisation cross-sections) to calculate the X-ray production rate as the Monte Carlo code PENELOPE 2018 [23] and its EPMA dedicated module PENEPMA [21]. PENEPMA is dedicated to the simulation of X-ray spectra and quantities of interest for microanalysis by EPMA. The default MACs used in BADGERFILM have been extracted from the PENELOPE database, which were calculated from the photoelectric cross section calculated by Sabbatucci and Salvat [24]. The default electron impact ionisation cross-sections are those of Bote and Salvat [25] and the atomic transition rates (used to calculate X-ray production cross-sections) are from the LLNL Evaluated Atomic Data Library [26]. These atomic parameters are also those used in PENELOPE. It should be noted that the electron impact ionisation cross-section models originally used in the calculation of the $\phi(\rho z)$-models are unchanged as they are intrinsically related to the good performance of the model. These parameters are only used to calculate absolute X-ray intensities or to determine MACs. In addition to these default models, other atomic parameters models can be selected, and experimental MAC values can be specified for a particular emitter, X-ray line and absorber.

Calculated compositions and film thicknesses are given with an uncertainty estimate based on the fitting algorithm and on the k-ratio uncertainty. If no uncertainty on the *k*-ratio was given by the user, a 5 % error on the value is assumed. Uncertainties associated with other variables, atomic parameters and matrix correction models are not considered. The calculated *k*-ratios, as well as the experimental ones, are plotted as a function of the accelerating voltage allowing the

user to easily evaluate the quality of the fit. The data can be saved in a BADGERFILM text file to be loaded at a later time. STRATAGEM files (version 6.2) can also be imported, enabling compatibility with STRATAGEM [27] and PROBE FOR EPMA [28]. The calculated results can easily be exported to a spreadsheet programme in a pre-formatted layout.

## *4. THIN FILM ANALYSIS*

BADGERFILM is an EPMA software dedicated to the determination of thin film thicknesses and composition. It uses the multi-voltage method where experimental *k*-ratios are measured at different accelerating voltages. We present below two test examples performed on (i) a thin film on a substrate, and (ii) a multi-layer specimen.

### *4.1. Thin film on substrate*

The simple case of the thickness determination of a carbon film deposited on a Si substrate is shown. Experimental C-Kα and Si-Kα *k*-ratios (relative to pure standards) were acquired by Llovet and Merlet [8] at multiple accelerating voltages ranging from 2 to 25 kV. Using the XPHI model as implemented in XFILM, these authors estimated the C film thickness to be 137 nm (assuming a carbon density of 2.2 g/cm$^3$). Using the PAP model and the PENELOPE MACs, BADGERFILM estimated the C film thickness to be 135.1 ± 1.7 nm, similar to the value obtained by Llovet and Merlet. Figure 5 shows the excellent agreement between the experimental *k*-ratios and the BADGERFILM calculated *k*-ratios.

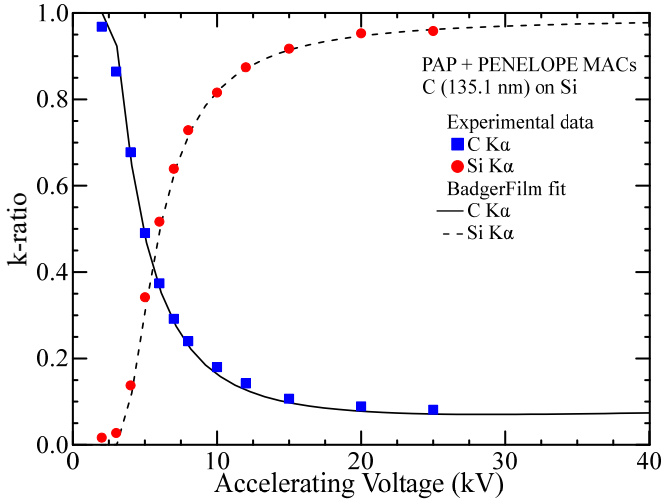


Figure 5. Determination of the thickness of a carbon film deposited on a Si substrate using the C and Si Kα *k*-ratios. Symbols are experimental *k*-ratios from [8]. Continuous and dashed lines are *k*-ratios calculated by BADGERFILM.

*4.2. Multi-layer specimens*

BADGERFILM iterates on the composition and thickness of the films (and substrate) to calculate theoretical *k*-ratios until they match the experimental *k*-ratios. Multi-layered specimen can easily be analysed using this technique. As shown in Fig. 6, the compositions and thicknesses of a bilayer of Ni-Cr/Fe-Gd-Pt on top of a Si substrate is determined using three accelerating voltages at 20, 25 and 30 kV. Experimental data acquired by Pouchou were extracted from [29]. Experimental *k*-ratios (relative to pure standards) for the Ni-Kα, Cr-Kα, Fe-Kα, Gd-Lα and Pt-Mα were processed by BADGERFILM using the PAP model and MACs extracted from the PENELOPE database. The obtained results are as follow: a 68.3 nm thick first layer with a composition of 14.4 wt% Ni and 85.6 wt% Cr, and a 24.0 nm thick second layer with a composition of 50.3 wt% Fe, 29.4 wt% Gd and 20.3 wt% Pt. These results are in excellent agreement with the original results of Pouchou obtained using STRATA (the ancestor of STRATAGEM), as well as with results obtained with other thin film analysis programmes and other thin film characterisation techniques, such as the Rutherford backscattering technique [16]. PENEPMA Monte Carlo simulation were also performed using the film thickness and composition found by BADGERFILM. Simulated *k*-ratios are in excellent agreement with the experimental *k*-ratios and the BADGERFILM calculated *k*-ratios (Fig. 6), supporting the good accuracy of the method.

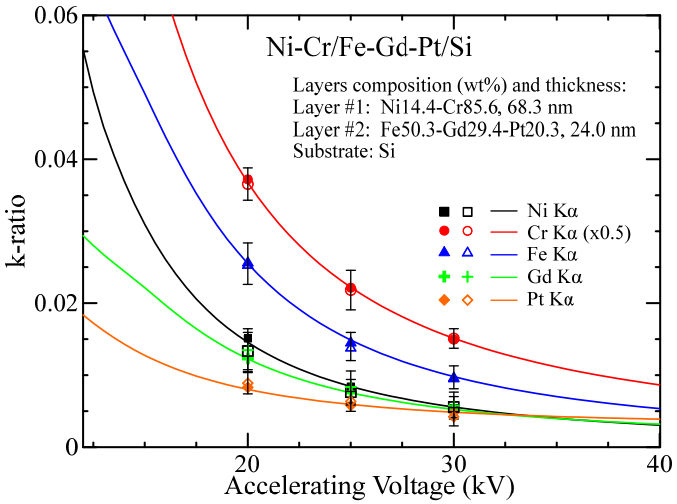


Figure 6. Determination of the compositions and thicknesses of a NiCr/FeGdPt/Si multi-layer specimen using the Ni-Kα, Cr-Kα, Fe-Kα, Gd-Lα and Pt-Mα *k*-ratios. Solid symbols are experimental *k*-ratios from [8]. Continuous lines are for *k*-ratios calculated by BADGERFILM. Open symbols are from PENEPMA simulations and the associated error bars correspond to a 3-sigma uncertainty.

## 5. *BULK SPECIMEN*

BADGERFILM is not only dedicated to the analysis of thin film samples but can also accurately quantify bulk specimens [15]. Oxygen is not always routinely measured, especially in geological materials, mainly because of spectral interferences (notably with EDS spectrometers), because of the difficulty of having a well characterised O standard (O is strongly absorbed by the coating of the standard and any uncertainty in the coating thickness will result in uncertainties in the quantification results) or simply to reduce the analysis time. In such situation, O is determined by stoichiometry relative to the other cations. BADGERFILM offers the possibility to quantify samples using O defined by stoichiometry as well as another element defined by stoichiometry relative to O. As an example, the quantification of a dolomite specimen, (ideal stoichiometric formula $CaMg(CO_3)_2$), can be done by only measuring Ca and Mg (and trace elements such as Fe and Sr if present) and by determining O by stoichiometry and C relative to O using a 1:3 atomic ratio. The correct appropriation of O and C is made during the matrix correction iterations, rather than after the calculations. This allows these elements to be fully accounted for in the matrix correction procedure and avoid any quantification bias that can result when these elements are added after the correction (Table 1).

Table 1. Elemental concentration (in wt. fraction) of a dolomite sample with O and C either determined by stoichiometry during the matrix correction procedure or not considered.

| | **Fe** | **Mn** | **Ca** | **Mg** | **O** | **C** | **Total** |
|---|---|---|---|---|---|---|---|
| with O, C | 0.0093 | 0.0014 | 0.2117 | 0.1252 | 0.5104 | 0.1277 | 0.9857 |
| no O, C | 0.0098 | 0.0015 | 0.2210 | 0.1222 | - | - | 0.3545 |
| error % | 5.4 | 7.1 | 4.4 | -2.4 | | | |

## 6. *MAC DETERMINATION*

BADGERFILM can also be used to determine MACs by using multi-voltage measurements on specimens of known composition and geometry (film thickness). The MAC for a given emitter, characteristic X-ray line and absorber is set as unknown, and the fitting algorithm will iterate on this unknown MAC value until the calculated and experimental *k*-ratios match. To illustrate this technique, the MAC of the Si Kα-line by Hf in $HfSiO_4$ can be estimated by recording the Si-Kα X-ray intensity at several accelerating voltages. The data were processed with BADGERFILM using the PAP $\phi(\rho z)$-model as well as MACs extracted from the PENELOPE database for the MACs other than the one of interest. As shown in Fig. 7, the MAC value found by BADGERFILM of 3,172 $cm^2/g$ is in good agreement with the value found by Donovan [28] of 3,477 $cm^2/g$. For comparison purpose, the values obtained from the FFAST [30] and MAC30 [31] theoretical MAC databases are given. We can observe large discrepancies between the experimental and theoretical MACs, indicating a need for a re-evaluation of some MACs, notably for low energy X-rays and for high Z absorbers (see Llovet *et al.* [32, 33], this meeting).

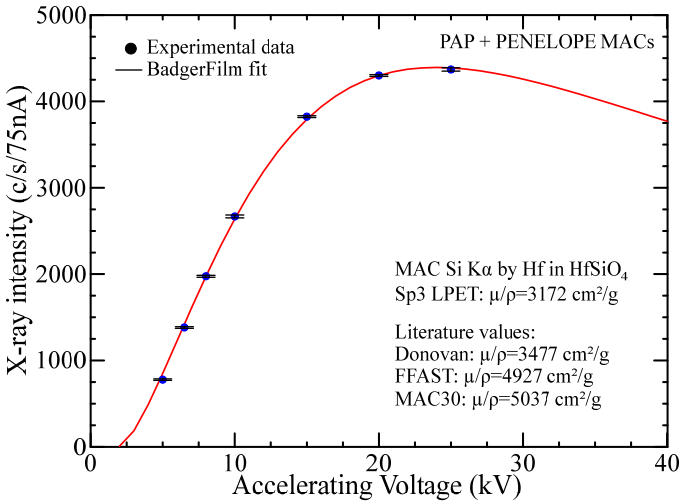


Figure 7. Determination of the Si-Kα by Hf MAC in $HfSiO_4$ by BADGERFILM. Symbols are experimental X-ray intensities. The continuous line is the result of the fitting by BADGERFILM using the PAP $\phi(\rho z)$-model and PENELOPE MACs. The obtained value is compared to experimental [28] and theoretical [30, 31] values form the literature.

## 7. *CONCLUSION*

BADGERFILM is a versatile, free and open-source EPMA analysis programme, for the quantification of multi-layered specimens, as well as bulk samples. The programme implements several $\phi(\rho z)$-models, MACs datasets, as well as atomic parameters. BADGERFILM was designed to be flexible and easily modifiable, to be adapted to new types of problems that EPMA users may encounter. The programme has been shown to give accurate thin film characterisation results when compared to other thin film programmes and other characterisation methods. BADGERFILM can be downloaded at the following address: https://github.com/Aurelien354/BadgerFilm.

## 8. *ACKNOWLEDGEMENTS*

Support for this research came from the National Science Foundation: EAR-1337156 (JHF), EAR-1554269 (JHF) and EAR-1849386 (JHF).

## 9. *REFERENCES*

[ 1] Llovet X, Moy A, Pinard P T and Fournelle J H 2020 *Prog. Mater. Sci.* **116** 100673
[ 2] Sweeney W E, Seebold R E and Birks L S 1960 *J. Appl. Phys.* **31** 1061-1064
[ 3] Hunger H-J 1988 *Scanning* **10** 65-72

[ 4] Dumelié N, Benhayoune H and Balossier G 2007 *J. Phys. D. Appl. Phys.* **40** 2124-2131
[ 5] Lavrent'ev Y G, Korolyuk V N and Usova L V 2004 *J. Anal. Chem.* **59** 600-616
[ 6] Pouchou J-L and Pichoir F 1991 Quantitative analysis of homogeneous or stratified microvolumes applying the model "PAP". in: *Electron probe quantitation*. (Heinrich K F J and Newbury D E; Eds.) [New York: Springer] 31-75
[ 7] Merlet C 1995 *A new quantitative procedure for stratified samples in EPMA*. in: Proc. 29th Ann. Conf. Microbeam Analysis Society. (Etz E S; Ed.) [VCH Publishers, Inc.] 203-204
[ 8] Llovet X and Merlet C 2010 *Microsc. Microanal.* **16** 21-32
[ 9] Waldo R A 1988 An iteration procedure to calculate film compositions and thicknesses in electron-probe microanalysis. in: *Microbeam analysis*. (Newbury D E; Ed.) [San Francisco: San Francisco Press, Inc.] 310-314
[10] Levenberg K 1944 *Appl. Math.* **2** 164-168
[11] Marquardt D 1963 *J. Soc. Ind. Appl. Math.* **11** 431-441
[12] Pouchou J and Pichoir F 1984 *J. Phys.* **45** 17-20
[13] Pouchou J and Pichoir F 1984 *J. Phys.* **45** 47-50
[14] Castaing R 1951 *Application des sondes electroniques a une méthode d'analyse ponctuelle chimique et cristallographique*. Office national d'études et de recherches aéronautiques (Paris), ISSN 0369-7622 ; no. 55
[15] Moy A and Fournelle J 2021 *Microsc. Microanal.* **27** 266-283
[16] Moy A and Fournelle J 2021 *Microsc. Microanal.* **27** 284-296
[17] Merlet C 1992 Quantitative electron probe microanalysis: New accurate Φ(ρz) description. in: *Electron microbeam analysis*. (Boekestein A and Pavićević M K; Eds.) [Vienna, Austria: Springer] 107-115
[18] Merlet C 1994 *Mikrochimica Acta* **114-115** 363-376
[19] Hunger H-J and Rogaschewski S 1986 *Scanning* **8** 257-263
[20] Small J A, Leigh S D, Newbury D E and Myklebust R L 1987 *J. Appl. Phys.* **61** 459-469
[21] Llovet X and Salvat F 2017 *Microsc. Microanal.* **23** 634-646
[22] Pouchou J L and Pichoir F M A 1988 in: *Microbeam analysis*. (Newbury D E; Ed.) [San Francisco: San Francisco Press, Inc.] 319-324
[23] Salvat F 2019 *PENELOPE 2018: A code system for Monte Carlo simulation of electron and photon transport*. OECD Data Bank, NEA/MBDAV/R(2019)1
[24] Sabbatucci L and Salvat F 2016 *Radiat. Phys. Chem.* **121** 122-140
[25] Bote D and Salvat F 2008 *Phys. Rev. A - Atom. Molec. Opt. Phys.* **77** 1-24
[26] Perkins S T, Cullen D E, Chen M H, Rathkopf J, Scofield J and Hubbell J H *1991 Tables and graphs of atomic subshell and relaxation data derived from the LLNL Evaluated Atomic Data Library (EADL), Z = 1-100*. [Livermore, CA: LLNL]
[27] *STRATAGem version 6.2*. SAMx, 4, rue Galilée, 78280 Guyancourt, France
[28] Donovan J J, Kremser D, Fournelle J and Goemann K 2021 *Probe for EPMA v. 12.9.5 User's guide and reference*. [Eugene, OR: Probe Software, Inc.]

[29] Pouchou J-L 1993 *Anal. Chim. Acta* **283** 81-97
[30] Chantler C T, Olsen K, Dragoset R A, Chang J, Kishore A R, Kotochigova S A and Zucker D S 2005 *X-ray form factor, attenuation and scattering tables (version 2.1)*. [Gaithersburg, VA: National. Institute for Standands and Technology]
[31] Heinrich K F J 1987 Mass absorption coefficients for electron probe microanalysis. in: *Proc. ICXOM XI*. (Brown J J D and Packwood R H; Eds.) 67-119
[32] Llovet X, Pöml P, Moy A and Fournelle J H 2023 Soft X-ray EPMA: choosing the right MACs. in: *Book of Tutorials and Abstracts of the EMAS 2023 Workshop*. [Zürich, Switzerland: European Microbeam Analysis Society eV (EMAS)]
[33] Llovet X, Pöml P, Moy A and Fournelle J H 2023 *Microsc. Microanal.* **29** (in press) https://doi.org/10.1093/micmic/ozac045